Article

Intelligent Ball Bearing Fault Diagnosis by using Fractional Lorenz Chaos Extension Detection Method with Acceleration Sensor

An-Hong Tian [1], Cheng-Biao Fu [1], Yu-Chung Li [2] and Her-Terng Yau [3,*]

[1] College of Information Engineering, Qujing Normal University, Qujing 655011, China; fucb@mail.qjnu.edu.cn (C.-B.F.); tianah@mail.qjnu.edu.cn (A.-H.T.)
[2] Department of Mechanical Engineering, National Cheng Kung University, 1 University Road, Tainan City 701, Taiwan; a238966777@gmail.com
[3] Department of Electrical Engineering, National Chin-Yi University of Technology, Taichung 41170, Taiwan
* Correspondence: pan1012@ms52.hinet.net or htyau@ncut.edu.tw; Tel.: +886-4-23924505

Abstract: In this study we used a non-autonomous Chua's Circuit, and the fractional Lorenz chaos system together with a detection method from Extension theory to analyze the voltage signals. The measured bearing signals by acceleration sensor were introduced into the master and slave systems through a Chua's Circuit. In a chaotic system minor differences can cause significant changes that generate dynamic errors, and extension matter-element models can be used to judge the bearing conditions. Extension theory can be used to establish classical and sectional domains using the dynamic errors of the fault conditions. The results obtained were compared with those from Discrete Fourier Transform analysis, Wavelet analysis and an integer order chaos system. The diagnostic ratio showed the fractional order master and slave chaos system calculations. The results show that the method presented in this paper is very suitable for monitoring the operational state of ball bearing system to be superior to the other methods. The diagnosis ratio was better and there were other significant advantages such as low cost and few.

Keywords: Ball bearing; Fractional Lorenz chaos system; Extension theory; Chua's Circuit Fault diagnosis

1. Introduction

The ability to accurately monitor the state of wear and the performance[1-3] of ball bearings in machine tools is important for several reasons. The most serious being that an unexpected breakdown can cause irreparable damage to other parts of the machine. However, over the long term, wear in bearings will result in a loss of machining accuracy and poor performance will reduce the quality of the product. This makes monitoring of the state of bearings important for the early detection of problems so that timely replacement can be made.

Many studies have been made recently into various methods for the diagnosis of faults in ball bearings. The methods mainly used involve stator current signals[4-7] , audio signals[8,9] and vibration signals[10,11].. For the analysis of the signals, both Discrete Fourier[12] transform and Wavelet analysis[13,14] are most often utilized. Although Discrete Fourier Transform may acquire fault frequencies, locations and volumes, the analyses are relatively weak in a non-linear system[15] and time domain changes and precise judgment of ball bearing condition is not possible. In Wavelet analysis, the bearing frequency range fluctuates widely and there is no way of knowing if the chosen mother wavelets are the correct ones from amongst all the high and low frequency signals. Furthermore, sensors need to be added to measure the physical data to facilitate Wavelet transformation. This can be expensive and also result in many false judgments. In the normal state and fault state of a wavelet neural network[16,17] analysis, the fault states are classified according to the characteristics of the neural network acquired through Fourier transforms. However, the use of a

neural network requires a huge database of learned examples. Massive numbers of calculations are needed during the process and real-time detection of problems is impossible. Another problem is the accuracy of learned samples. Other comparative research[18] publications have been seen that utilize the same data base to identify bearing fault conditions, but their diagnosis ratios are unknown. Although the artificial immunity-based method is also utilized for bearing fault diagnosis and can find faults, the diagnosis ratio is not all that good. A good diagnosis ratio can be achieved using Extension theory integrated with a master and slave chaos system[19]. However, the dynamic error signals generated by the system need Fractal processing and the time needed may not be in line with expectations for real-time diagnosis. There is much room for improvement.

In this paper we have offered a new approach using synchronized fractional chaos processing to remove less characteristic signals and diagnose the current state of a ball bearing system simply by using the chaos characteristics. The amount of waveform data used can be down-sized with a consequent reduction of calculation time. A much better diagnosis ratio can also be achieved. The bearing system signals can be analyzed by Extension identification, and better order numbers can be chosen by observing the chaos synchronizing motion traces from different fractional orders.

2. CHUA'S CIRCUIT

The simple layout of Chua's Circuit[20] designed by Chua in 1983 The circuit has three active components: capacitors, inductors, resistors, and a nonlinear resistor. $R_L$is the Chua's Diode, as shown in Figure 1

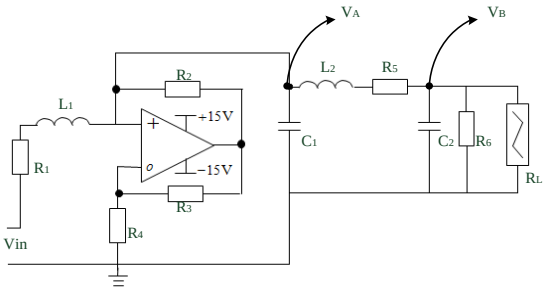

Figure 1. Diagram of Chua's Circuit

According to Kirchhoff's law, the Chua's Circuit's state equation is as (1):

$$\begin{cases} C_1 \dfrac{dV_{C1}}{dt} = -gV_{c1} + i_{L1} - i_{L2} \\ C_1 \dfrac{dV_{C2}}{dt} = i_{L1} - i_{RL} \\ L_1 \dfrac{di_{L1}}{dt} = -V_{C1} + i_{L1}R_1 + V_{in}\sin(2\pi k) \\ L_2 \dfrac{di_{L2}}{dt} = V_{C1} + V_{C2} + i_{L2}R_5 \end{cases} \tag{1}$$

Where k is a parameter corresponding to higher harmonics, and iRL is defined as (2).

$$i_{RL} = G_a V_{C2} + \frac{1}{2}(G_b - G_a)\left[\left|V_{C2} + E_a\right| - \left|V_{C2} - E_a\right|\right] \tag{2}$$

Wherein G_a and G_b are the slopes, and E_a is the breakpoint

In this study a non-autonomous Chua's Circuit is utilized to capture ball bearing characteristic signals, to capture V_a and V_b wave form characteristics, to introduce the voltage wave form characteristics into chaos for an extension matter-element model, and finally to utilize the extension algorithm to judge if a bearing is faulty.

3. Experiment System

This paper has used simulation data from the US Case Western Reserve University Bearing Data Center[21], and the database provides experiment data for both normal and faulty ball bearings. **Figure 2** shows the experimental platform utilized by the data base. It consists of a 2HP motor, encoders, a shaft for supporting the bearings, and a dynamometer. Faults are introduced in the bearings by electro-discharge machining (EDM) on the inner ring rollway, outer ring rollway and the roll ball of 0.007, 0.0014 and 0.0021-inch diameter to a depth of 0.011 inch for mono point faults. Loads were applied in the range of 0-3 HP (horse-power) for testing. Please refer to Table 1 for detailed specifications. Accelerometers were used to collect data from faulty and normal bearings. These were installed at the ends of the actuator and motor case at a 12 o'clock position. The collected data was processed and stored using MATLAB.

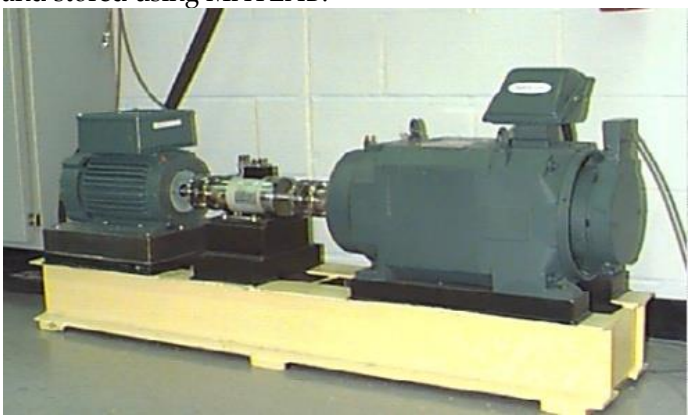

Figure **2.** Ball bearing experiment platform

Table 1. Types of ball bearing faults.

Sampling frequency(Hz)	Motor load(HP)	Fault single point diameter(inches)	Fault single point depth(inches)	Fault condition
12k 48k	0 1 2 3	0.007 0.014 0.021	0.011	Normal ball bearing fault inner ring fault outer ring fault

4. Chaos Theory

Chaos theory deals with the behavior of nonlinear dynamic systems which are very sensitive to small changes in initial conditions. Motion traces can be created due to chaos attractors which are ordered but non-periodic. Original motion signals may be small, but will result in the output of much bigger signals. In the chaos signal synchronizing systems, we may call a two chaos system a Master (MS) and Slave (SS) system. Two systems with different initial values will result in two motion traces, one for each of the different chaos phenomenon. However, the master-slave systems can be synchronized by adding controllers on the slave system to track the master. This section will describe the design process of the fractional-order chaotic self-synchronization of dynamic errors in detail. Table 2 presents the associated notation and definitions.

Table2. Nomenclature

Notation	Definition	Notation	Definition
X	The system states of master system	Γ( )	Gamma function
Y	The system states of slave system	a′, b′, c′	System parameters of fractional–order system
f	Nonlinear function	Φi	Dynamic error equation
U	Control input	g , h	The upper and lower limits of the classical domain
A	System parameter vector	r , s	The upper and lower limits of the joint domain
a, b, c	System parameters of Chen-Lee Chaos System	N	The name of a matter-element
e	System error state vector	ε	The characteristics of the matter-element
D	Differential operator	μ	The values corresponding to the characteristics
α	The value of differential order	Ω	The universe of discourse

The characteristic quantities adopted in this paper are subject to the size of the natural dynamic errors between the master and slave, and master/slave synchronizing systems. This means the master/slave systems mentioned here have not been designed with controllers, and the dynamic error conditions can be acquired simply by subtracting one from the other. The master-slave chaotic system is intended mainly to control the system state so that the desired state can be attained. The system consists of a master system (MS) and a slave system (SS) [15, 16], which are respectively expressed by equation (3)and equation (4):

$$\dot{X} = AX + f(X) \tag{3}$$

$$\dot{Y} = AY + f(Y) + U \tag{4}$$

Where $X \in R^N$ and $Y \in R^N$ are state vectors, A is an $N \times N$ system matrix, $f(X)$ and $f(Y)$ are non-linear vectors, and U is designed as a non-linear control term. To carry out signal processing, a non-linear chaotic system, such as a Lorenz system [22], with $N = 3$ is used. Take the Lorenz system for example[22], the Master-Slave dynamic equations are also listed as matrix formats as expression.

$$\begin{cases} \dot{x}_1 = \alpha(x_2 - x_1)x_1 \\ \dot{x}_2 = \beta x_1 - x_1 x_3 - x_2 \\ \dot{x}_3 = x_1 x_2 - \gamma x_3 \end{cases} \quad \begin{cases} \dot{y}_1 = \alpha(y_2 - y_1) \\ \dot{y}_2 = \beta y_1 - y_1 y_3 - y_2 \\ \dot{y}_3 = y_1 y_2 - \gamma y_3 \end{cases} \tag{5}$$

Wherein the dynamic error is defined as $e_1 = x_1 - y_1$, $e_2 = x_2 - y_2$, $e_3 = x_3 - y_3$ and $e = [e1, e2, e3]^T$, dynamic error statement function is calculated and matrix form statement is written as expression.

$$\begin{bmatrix} \dot{e}_1 \\ \dot{e}_2 \\ \dot{e}_3 \end{bmatrix} = \begin{bmatrix} -\alpha & \alpha & 0 \\ \beta & -1 & 0 \\ 0 & 0 & -\gamma \end{bmatrix} e + \begin{bmatrix} e_1 \\ e_2 \\ e_3 \end{bmatrix} + \begin{bmatrix} 0 \\ -e_1 e_3 \\ e_1 e_2 \end{bmatrix} \tag{6}$$

According to Grünwald-Letnikov's fractional order approximation, the statement can be expressed as (7)

$$D_e^{\pm\alpha} e^m \approx \frac{\Gamma(m+1)}{\Gamma(m+1\pm\alpha)} e^{m\pm\alpha} \tag{7}$$

where e is dynamic error, m is an arbitrary real number, and α is the selected desired phenomenon, as shown in Figure 3. Based on $|\alpha|$, the following two rules apply:

1. $0.00 < |\alpha| \le 0.20$: for quantification of arithmetic values and proportion-related applications

2. $0.20 < |\alpha| \le 1.00$: for the control of non-arithmetic values and classification applications

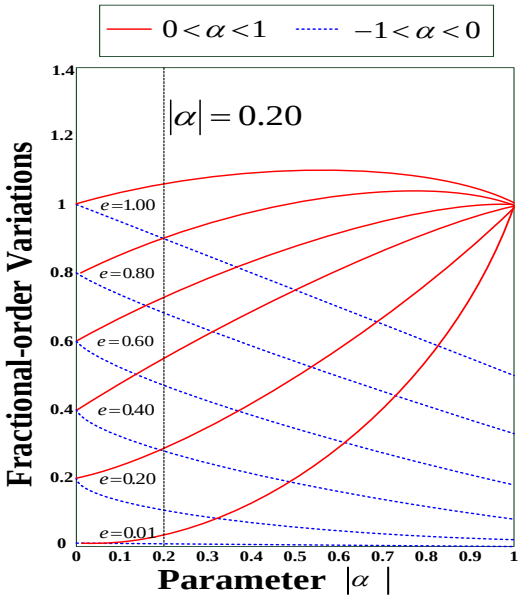

Figure 3. Dynamic error in response to fractional-order variation ($\alpha = \pm 0.02$, $m = 1$).

For expressing fractional changes, fractional order modifications on the first-order differential system can be expressed as equation (8).

Preprints (www.preprints.org) | NOT PEER-REVIEWED | Posted: 30 July 2018 doi:10.20944/preprints201807.0576.v1

Peer-reviewed version available at Sensors 2018, 18; doi:10.3390/s18093069

$$\frac{d}{dt}\frac{d^{-\alpha}}{dt^{-\alpha}} \approx A(e)\frac{d^{-\alpha}}{dt^{-\alpha}}\begin{bmatrix} e_1^1 \\ e_2^1 \\ e_3^1 \end{bmatrix} + \frac{d^{-\alpha}}{dt^{-\alpha}}\begin{bmatrix} e_1^0 \\ -e_1e_3 \\ e_1e_2 \end{bmatrix}$$

$$\Rightarrow \begin{bmatrix} D^q e_1 \\ D^q e_2 \\ D^q e_3 \end{bmatrix} \approx \begin{bmatrix} -\alpha' & \alpha' & 0 \\ \beta' & 0 & 0 \\ 0 & 0 & -\gamma' \end{bmatrix}\begin{bmatrix} e_1^{1+\alpha} \\ e_2^{1+\alpha} \\ e_3^{1+\alpha} \end{bmatrix} + \begin{bmatrix} \frac{\Gamma(1)e_1^{\alpha}}{\Gamma(1+\alpha)} \\ \frac{\Gamma(1)e_1e_3e_2^{\alpha}}{\Gamma(1+\alpha)} \\ \frac{\Gamma(1)e_1e_2e_3^{\alpha}}{\Gamma(1+\alpha)} \end{bmatrix} \tag{8}$$

Where $q=(1-\alpha)$, $0<q\le 1$ is to achieve fractional order, and $\Gamma(\bullet)$ is a gamma function. $\Gamma(1)=\Gamma(2)=1$, wherein the system parameters $\dot{\alpha}$, $\dot{\beta}$ and $\dot{\gamma}$ are non-zero constants. They must therefore be converted into an expression such as equation (9).

$$\alpha' = \frac{\alpha\Gamma(2)}{\Gamma(2+\alpha)}, \beta' = \frac{\beta\Gamma(2)}{\Gamma(2+\alpha)}, \gamma' = \frac{\gamma\Gamma(2)}{\Gamma(2+\alpha)} \tag{9}$$

The chaos system used here employs a nonlinear Chua's Circuit with signal transform inputs VA and VB and e1, e2, and e3 are used to make trace diagrams of the phase domain. The important characteristics are the four bearing state signals: normal signal, bearing fault, inner ring fault and outer ring fault, and the dynamic errors are:

$$\begin{cases} e_1[i] = x[i] - y[i] \\ e_2[i] = x[i+1] - y[i+1] \\ e_3[i] = x[i+2] - y[i+2] \end{cases} \tag{10}$$

Where x and y are the V_A and V_B signals.

The foregoing system is used in this study as the chaotic system for converting ball bearing vibration signals. The data of the aforesaid Center are collected in a way in which all the data on its website that correspond to the sampling frequency of 48K are adopted. The original data adopted include a total of about 240000 entries, in which the 0th-48000th entries correspond to the 1-second transient state caused by motor startup and therefore are not taken into consideration. The remaining data are divided into two parts, each of a size of about 96000 entries. One part is used for data analysis, and the other, for verifying the results. The important characteristics are formed according to the trajectories of the dynamic errors $e1, e2, e3$ on the phase planes and signals representing the four different ball bearing states, namely normal state, ball fault, inner race fault, and outer race fault. In this study the dynamic error signals were acquired by introducing V_A and V_B as the test signals into the master/slave system, and the dynamic error signals e2 and e3 were used to plot dynamic trace diagrams. The dynamic trajectories of each state can be observed, allowing us to establish the matter-element model in the extension theory for identifying the output signals of the monitoring system.

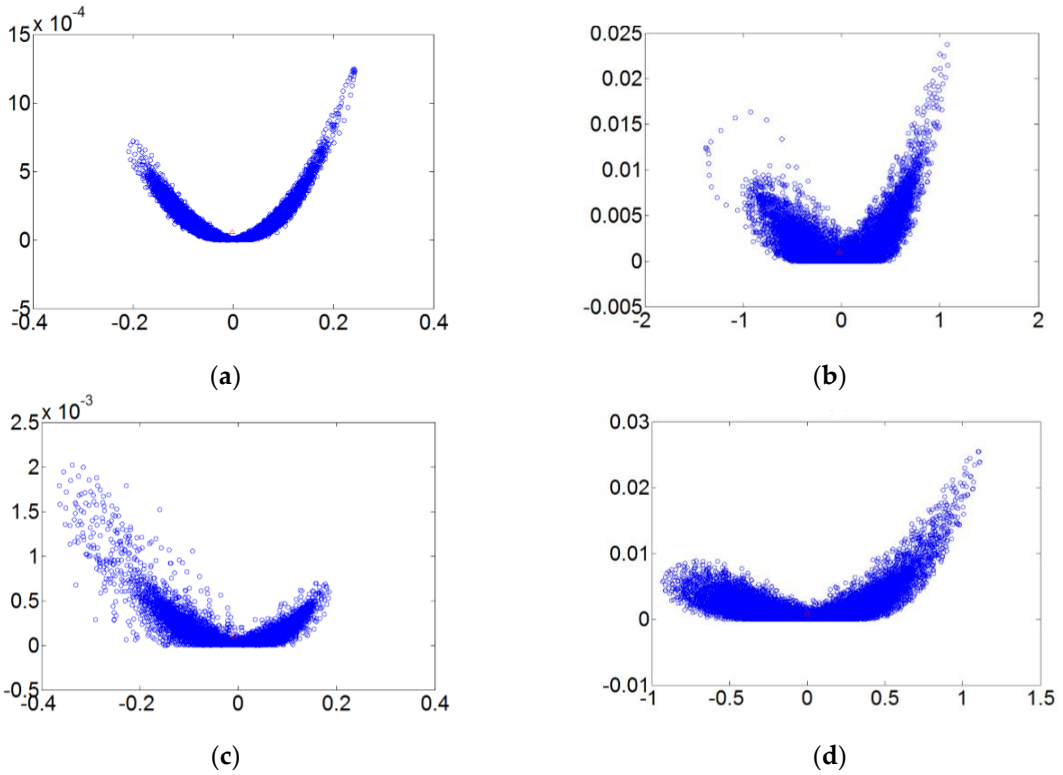

Figure 4. The order 1 fault dynamic error trace diagrams for all fault diameters. (a)Normal state; (b) Fault diameter=0.007 (c) Fault diameter=0.014; (d) Fault diameter=0.021

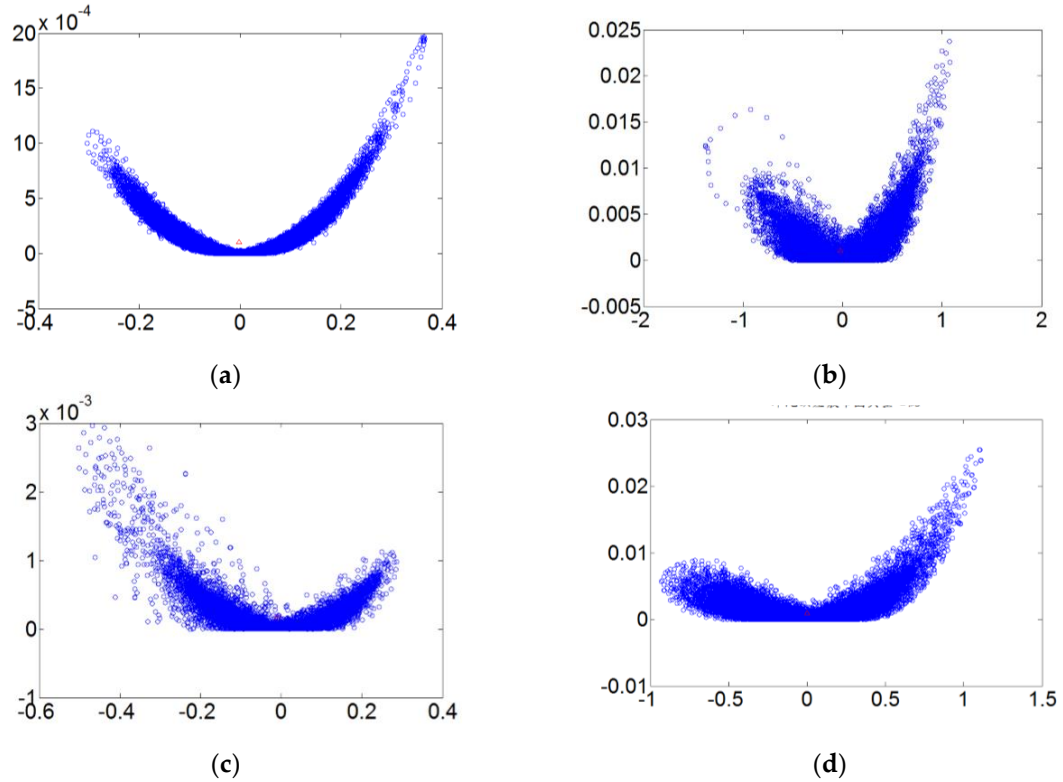

Figure 5. The order 0.9 fault dynamic error trace diagrams for all fault diameters. (a)Normal state; (b) Fault diameter=0.007 (c) Fault diameter=0.014; (d) Fault diameter=0.021

Preprints (www.preprints.org) | NOT PEER-REVIEWED | Posted: 30 July 2018 doi:10.20944/preprints201807.0576.v1

Peer-reviewed version available at Sensors 2018, 18; doi:10.3390/s18093069

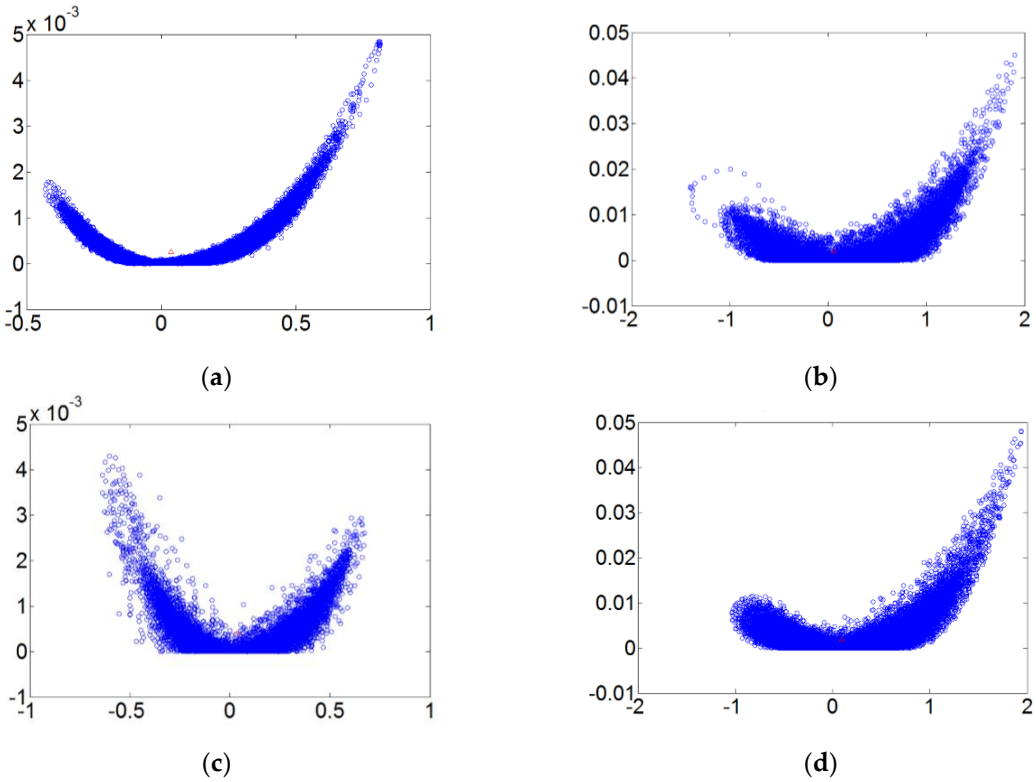

Figure 6. The order 0.7 fault dynamic error trace diagrams for all fault diameters. (a)Normal state; (b) Fault diameter=0.007 (c) Fault diameter=0.014; (d) Fault diameter=0.021

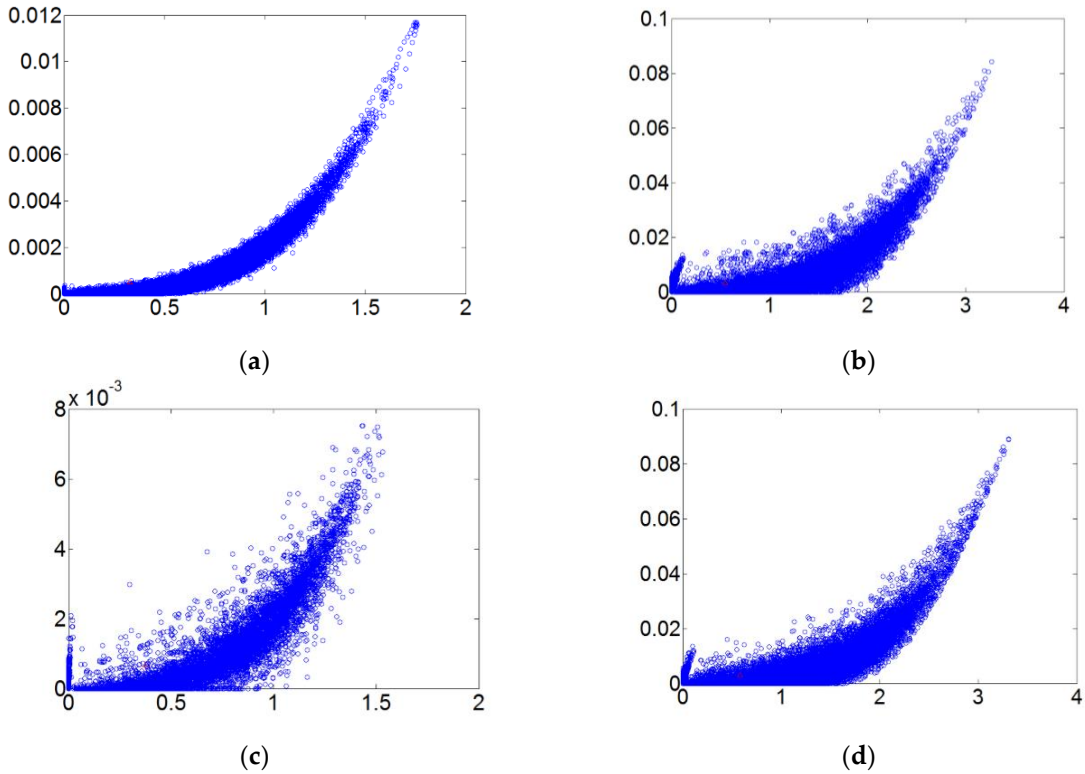

Figure 7. The order 0.5 fault dynamic error trace diagrams for all fault diameters. (a)Normal state; (b) Fault diameter=0.007 (c) Fault diameter=0.014; (d) Fault diameter=0.021

Preprints (www.preprints.org) | NOT PEER-REVIEWED | Posted: 30 July 2018 doi:10.20944/preprints201807.0576.v1

Peer-reviewed version available at Sensors 2018, 18; doi:10.3390/s18093069

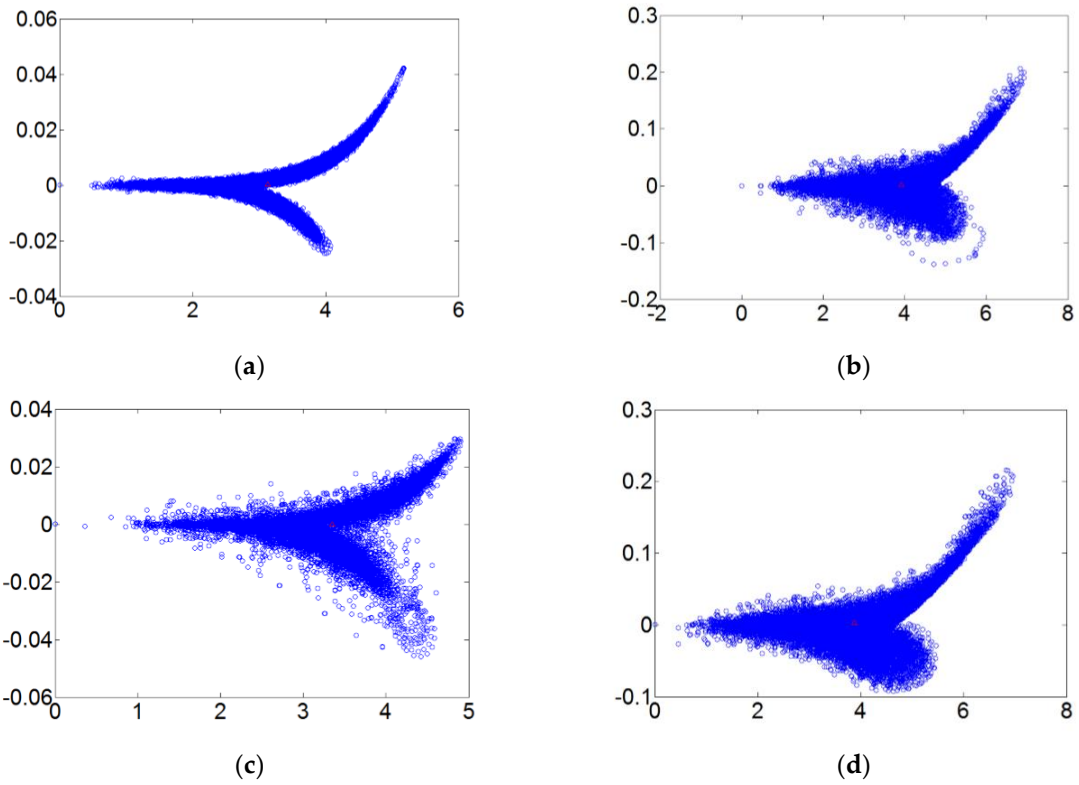

Figure 8. The order 0.3 fault dynamic error trace diagrams for all fault diameters. (a)Normal state; (b) Fault diameter=0.007 (c) Fault diameter=0.014; (d) Fault diameter=0.021

Figure 4 refers to the fault diameters 0.007, 0.014, 0.021 inches and normal signals, and have been substituted using the integer order Chaos system to manage the ball bearing dynamic error diagrams. Under the integer order Chaos system, the dynamic errors of different states would be too concentrated in the same regions, and the characteristics would not be obvious. This means misjudgments could easily occur during calculations of the dynamic error distributions of the Extension theory matter-element models and such order numbers are unsuitable for signal processing by this system. **Figure 5 – Figure 8** refer to the dynamic error trace diagrams in which the fractional order chaos system is used for processing the ball bearing signal. According to the simulation results for the fault diameters of 0.007, 0.014 and 0.021 inches in comparison to the order 0.9, order 0.7, order 0.5 and order 0.3 order of the integer order chaos system, the results show that the dynamic errors among the states are relatively more decentralized, and the trace diagram for the order 0.3 is of relatively more obvious characteristic difference such that during the calculation of the dynamic error distribution, it is able to yield excellent identification result; therefore, order 0.3 is more suitable for processing signal in this system. Figure 9 shows a flow chart of the system of the present research.

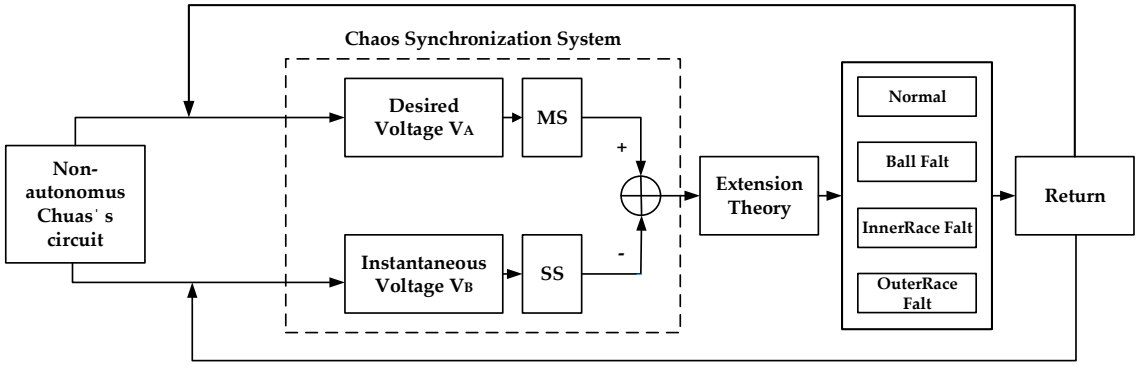

Figure 9. Ball bearing diagnosis system flow chart

5. Extension Theory

The extension theory [22] involves observing the different states of objects, seeking the regularity of the states by way of their extensibility, and deriving the characteristics of the states from mathematical operations. The extension theory can be generally divided into two parts: the matter-element model and the extension set. By using the matter-element model and the extension set, objects can be quantified and planned according to their correlation with one another, messages of the objects can be described with ease, and the range of a fuzzy set can be extended from $<0,1>$ to $<-\infty,\infty>$. Figure 10 schematically shows a fuzzy set and an extension set. For a more detailed description of the matter-element theory and the extension set, please refer to references [23] and [24].

(1) Matter-element theory

The core of the matter-element theory is to study such properties of matter-elements as extensibility, change, and transformation. When analyzing the phenomena of various objects, the objects can be distinguished by their characteristics, which clearly indicate the differences between the objects. For example, the differences in form, position, and mode between the objects can be expressed with mathematical values, or more particularly with the following mathematical matrix(11):

$$\phi = (N, \varepsilon, \mu) \tag{11}$$

where N is the name of a matter-element, ε is the characteristics of the matter-element, and μ is values corresponding to the characteristics. If an object has n characteristics, the characteristic vector can be expressed by, and the corresponding value vector, by. This matter-element is referred to as an n-dimension matter-element.

When the characteristic values are distributed in a certain range, the range is known as the classical domain and is included in a joint domain. Assume the intervals $F_0 =< g,h >$ and $F =< r,s >$, where: $F_0 \in F$, g and h are respectively the upper and lower limits of the classical domain, and r and s are respectively the upper and lower limits of the joint domain.

(2) Extension sets

Extension mathematics has extension sets and extension correlation functions at its core and serves to extend a specific set into a range of continuous values $<-\infty,\infty>$ and express the properties of an object via a correlation function. An extension set is a set of real numbers of the range $<-\infty,\infty>$ and expresses the extent to which an object has the features of interest. The concept and definitions of an extension set are as follows:

Assume Ω is the universe of discourse, and any element ω in Ω (i.e., $\omega \in \Omega$) has a corresponding real number (i.e., $K(\omega) \in <-\infty,\infty>$). Then, an extension set can be defined by equation(12):

$$\Pi = \Pi^{+} \cup \Pi^{0} \cup \Pi^{-} \tag{12}$$

where Π^+, Π^0, and Π^- are the positive domain, zero domain, and negative domain of the extension set respectively, as shown in Figure 10and expressed by equations (13),(14) and (15) respectively:

$$\Pi^+ = \{(\omega, y) | \quad \omega \in \Omega \quad , \quad y = K(\omega) > 0\} \tag{13}$$

$$\Pi^0 = \{(\omega, y) | \quad \omega \in \Omega \quad , \quad y = K(\omega) = 0\} \tag{14}$$

$$\Pi^- = \{(\omega, y) | \quad \omega \in \Omega \quad , \quad y = K(\omega) < 0\} \tag{15}$$

As can be seen in Figure 10, the closer an object under test is to the classical domain, the greater the value of the correlation function, and, as indicated by the correlation function, the better the object's data fall into that specific class. Conversely, the farther an object under test is from the classical domain, the smaller the value of its correlation function, and, as indicated by the correlation function, the more poorly the object's data fall into that specific class.

(3) A matter-element model for use with the extension theory

When we establish a mathematical model for a problem to be solved, the problem is idealized, which gives rise to the question of whether the mathematical model we established is different from the problem itself. To deal with this issue, the extension theory makes use of a matter-element model. In extension we refer to an object as N, its characteristics as ε, and the corresponding values as μ. These three elements are known as the three essential factors of a matter-element and can be used to describe the object. When an object has multiple characteristics, it can be expressed by equation (16):

$$\phi = \begin{bmatrix} N & \varepsilon_1 & \langle \mu_1 \rangle \\ & \varepsilon_2 & \langle \mu_2 \rangle \\ & \cdots & \cdots \\ & \varepsilon_n & \langle \mu_n \rangle \end{bmatrix} \tag{16}$$

Conventionally, classification by the condition equations is rather intuitive: a point under test that falls within the range of a certain condition is classified as in that particular fault state. If a point under test does not fall into any condition, the conventional condition-based classification approach will be unable to identify the fault state correctly: that is to say, the system is very likely to produce a wrong diagnosis. The greatest difference between the extension theory and the conventional condition-based classification method (i.e. fuzzy theorem) is that the former emphasizes the degree of correlation and applies a concept similar to distance. Based on the extension theory, the system will automatically calculate and determine to which fault state the point under test is closest (i.e., has the smallest "distance") and thereby diagnose the point as having that kind of fault. Thus, errors in system diagnosis are prevented, and the diagnosis rate is increased.

The extension theory is used in this study as the means of identification of the back-end detection system of the FOCLCS. More specifically, the current state of ball bearing signals is classified by

observing the degree of correlation, for the greater the value of the correlation function is, the closer the matter-element under test is to the classical field, and the better the objects fall within the class of the classical field.

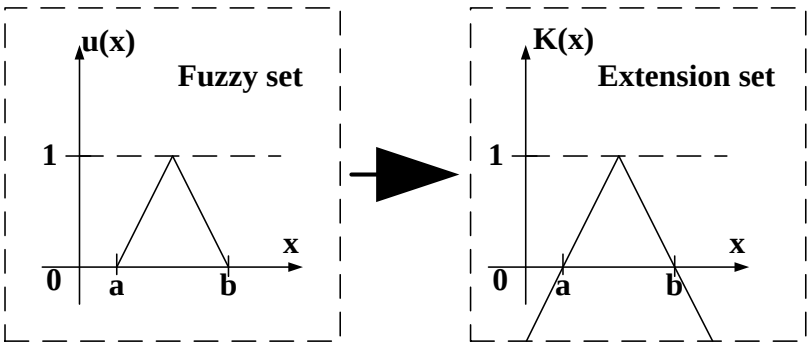

(a)

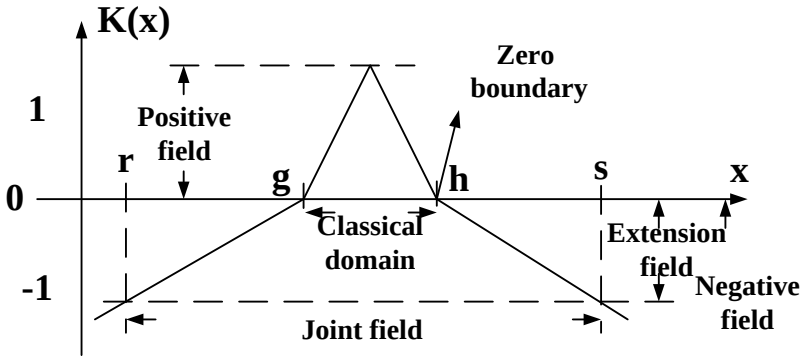

(b)

Figure 10. Different of Fuzzy set and Extension set. (a)Schematic drawings of a fuzzy set to an extension set. (b) explanatory diagram of extension set.

6. Experiment Results

The fractional Lorenz chaos synchronous dynamic error system was utilized to make the ball bearing signal transforms. Dynamic trace diagrams of e1, e2 and e3 have been observed. The different states provided by the experiments data base include normal, outer ring, roll ring and inner ring faults. Extension matter-element models were designed for distinguishing intelligent monitoring system output which works on the base of a 48k(Hz) sampling rate and a one second data volume formed from observation of important characteristics of different state dynamic errors e2 and e3 in dynamic error diagrams.

In the establishment of the extension matter-element model, four characteristic items, a_1, a_2, x and y have been established as a basis for judgment of the state of a ball bearing. a_1 represents the left-half distribution area of the horizontal axis of the dynamic error trace diagram, a_2 the right-half distribution area of the horizontal axis of the dynamic error trace diagram, and x stands for the left-half distribution area of the dynamic error trace diagram, and y stands for the right-half distribution area of the dynamic error trace diagram Expression (17) is the fault matter-element model of a ball bearing at 0HP for all diameters.

Preprints (www.preprints.org) | NOT PEER-REVIEWED | Posted: 30 July 2018 doi:10.20944/preprints201807.0576.v1

Peer-reviewed version available at Sensors 2018, 18; doi:10.3390/s18093069

$$\begin{bmatrix} Normal & \alpha_1 & [0,2] \\ & \alpha_2 & [2,4] \\ & x & [-0.01,0.05] \\ & y & [-0.01,0.03] \end{bmatrix} \begin{bmatrix} 0.007 & \alpha_1 & [0,2] \\ & \alpha_2 & [2,4] \\ & x & [-0.05,0.045] \\ & y & [-0.09,0.15] \end{bmatrix}$$
$$\begin{bmatrix} 0.014 & \alpha_1 & [0,2] \\ & \alpha_2 & [2,4] \\ & x & [-0.02,0.01] \\ & y & [-0.021,0.02] \end{bmatrix} \begin{bmatrix} 0.021 & \alpha_1 & [0,2] \\ & \alpha_2 & [2,4] \\ & x & [-0.05,0.03] \\ & y & [-0.05,0.15] \end{bmatrix} \quad (17)$$

The matter - element model established in this paper has four characteristics, each having a 0.25 weight setting. Each characteristic goes through Extension calculations and is accurately identified for ball bearing condition. In this paper the discrete Fourier transform, wavelet packet analysis and different order ranking of fractional chaos systems and other methods have been performed to identify random data. The statistical method used collected data on each state from 20 ball bearings and this was used to calculate the likelihood of accurate judgment. An examination of Figure 5-Figure 8 clearly shows that the order 0.3 Fractional Lorenz chaos system was superior to other methods and other orders. In addition, another advantage is that only vibration signals need to be collected for processing and the costs of the sensors needed can be minimal. **Figure 11** shown the accuracy of result for each method.

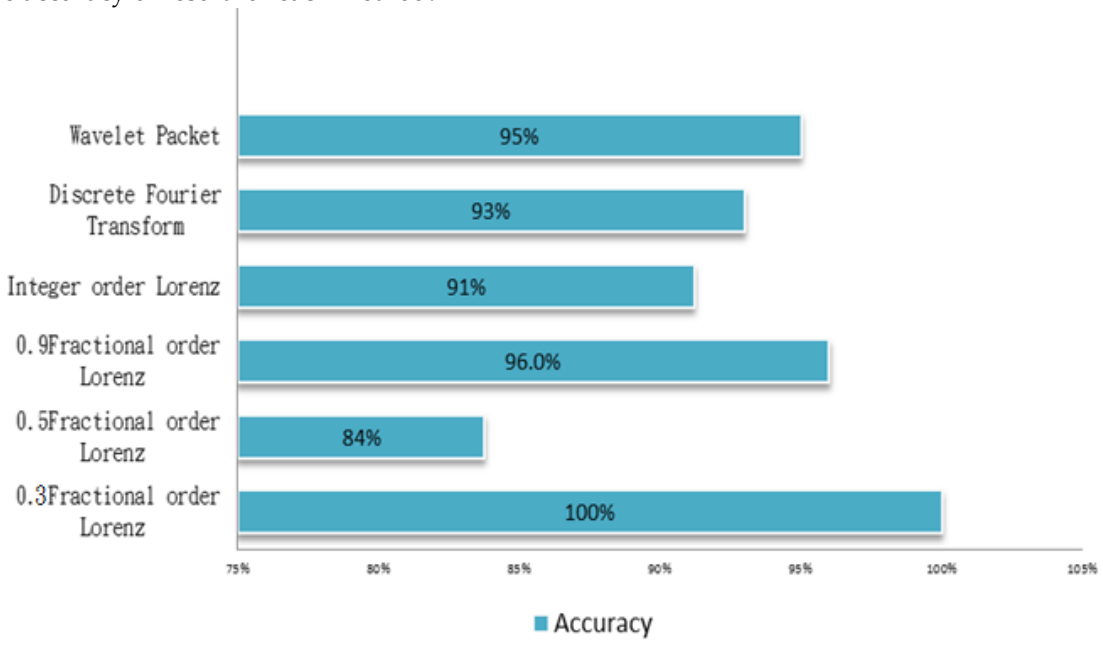

Figure 11. Chart of diagnosis accuracy with different method.

7. Conclusion

In this paper a method was presented for the evaluation of faults in ball bearings that integrates fractional order chaos synchronization dynamic error and Extension theory. Implementation of such a ball bearing intelligent state monitoring system can be done using the LabVIEW human-machine interface. The results of our experiments show the method to be useful and it has some distinct advantages in that cost is low because only one sensor is needed, calculations can be made quickly, and the accuracy of diagnosis is good. This method can be used to monitor the ball bearings in every part of a machine tool. Such an intelligent system would detect problems fast and accurately making it possible for faulty bearings to be found and replaced before the event of a breakdown. This will improve the overall efficiency of any machine tool installation.

This system can record and store captured signals and diagnosis results. If it could be integrated with EtherCAT in the future, it might be helpful in several ways. For example, the data could be uploaded to the cloud and be immediately available for other users anywhere. Such a database would be extremely useful as a check and for the review and evaluation, or the improvement, of existing methods. It would certainly help the development of Industry 4.0.

Acknowledgments: The authors would like to thank the National Science Council of the Republic of China, Taiwan, for financially supporting this research under Contract No. MOST 104-2221-E-167-001.

Conflicts of Interest:
The authors declare no conflicts of interest.

References

1. Sun, J.; Wang, C.; Le, Y. Designing and experimental verification of the axial hybrid magnetic bearing to stabilization of a magnetically suspended inertially stabilized platform. *IEEE/ASME Transactions on Mechatronics* **2016**, *21*, 2881-2891.
2. Le, Y.; Wang, K. Design and optimization method of magnetic bearing for high-speed motor considering eddy current effects. *IEEE/ASME Transactions on Mechatronics* **2016**, *21*, 2061-2072.
3. Zhou, L.; Li, L. Modeling and identification of a solid-core active magnetic bearing including eddy currents. *IEEE/ASME Transactions on Mechatronics* **2016**, *21*, 2784-2792.
4. Leite, V.C.M.N.; Silva, J.G.B.d.; Veloso, G.F.C.; Silva, L.E.B.d.; Lambert-Torres, G.; Bonaldi, E.L.; Oliveira, L.E.d.L.d. Detection of localized bearing faults in induction machines by spectral kurtosis and envelope analysis of stator current. *IEEE Transactions on Industrial Electronics* **2015**, *62*, 1855-1865.
5. Iorgulescu, M.; Beloiu, R. In *Faults diagnosis for electrical machines based on analysis of motor current*, 2014 International Conference on Optimization of Electrical and Electronic Equipment (OPTIM), 22-24 May 2014, 2014; pp 291-297.
6. Cui, L.; Liu, Z.; Fengxing, Z.; Cheng, G. In *Application of generalized demodulation in bearing fault diagnosis of inverter fed induction motors*, Proceeding of the 11th World Congress on Intelligent Control and Automation, June 29 2014-July 4 2014, 2014; pp 2328-2333.
7. Esfahani, E.T.; Wang, S.; Sundararajan, V. Multisensor wireless system for eccentricity and bearing fault detection in induction motors. *IEEE/ASME Transactions on Mechatronics* **2014**, *19*, 818-826.
8. Kang, M.; Kim, J.; Wills, L.M.; Kim, J.M. Time-varying and multiresolution envelope analysis and discriminative feature analysis for bearing fault diagnosis. *IEEE Transactions on Industrial Electronics* **2015**, *62*, 7749-7761.
9. Wang, J.; He, Q.; Kong, F. Adaptive multiscale noise tuning stochastic resonance for health diagnosis of rolling element bearings. *IEEE Transactions on Instrumentation and Measurement* **2015**, *64*, 564-577.
10. Junbo, T.; Weining, L.; Juneng, A.; Xueqian, W. In *Fault diagnosis method study in roller bearing based on wavelet transform and stacked auto-encoder*, The 27th Chinese Control and Decision Conference (2015 CCDC), 23-25 May 2015, 2015; pp 4608-4613.

11. Harmouche, J.; Delpha, C.; Diallo, D. Improved fault diagnosis of ball bearings based on the global spectrum of vibration signals. *IEEE Transactions on Energy Conversion* **2015**, *30*, 376-383.
12. Yamahata, C.; Sarajlic, E.; Krijnen, G.J.M.; Gijs, M.A.M. Subnanometer translation of microelectromechanical systems measured by discrete fourier analysis of ccd images. *Journal of Microelectromechanical Systems* **2010**, *19*, 1273-1275.
13. Zhang, Z.; Wu, J.; Ma, J.; Wang, X.; Zhou, C. In *Fault diagnosis for rolling bearing based on lifting wavelet and morphological fractal dimension*, The 27th Chinese Control and Decision Conference (2015 CCDC), 23-25 May 2015, 2015; pp 6351-6354.
14. Zhang, W.; Zhu, H.; Yang, Z.; Sun, X.; Yuan, Y. Nonlinear model analysis and "switching model" of ac–dc three-degree-of-freedom hybrid magnetic bearing. *IEEE/ASME Transactions on Mechatronics* **2016**, *21*, 1102-1115.
15. Mohanty, S.; Gupta, K.K.; Raju, K.S. In *Multi-channel vibro-acoustic fault analysis of ball bearing using wavelet based multi-scale principal component analysis*, 2015 Twenty First National Conference on Communications (NCC), Feb. 27 2015-March 1 2015, 2015; pp 1-6.
16. Jiang, L.; Fu, X.; Cui, J.; Li, Z. In *Rolling element bearing fault diagnosis using recursive wavelet and som neural network*, 2013 25th Chinese Control and Decision Conference (CCDC), 25-27 May 2013, 2013; pp 4691-4696.
17. Schmitt, H.L.; Silva, L.R.B.; Scalassara, P.R.; Goedtel, A. In *Bearing fault detection using relative entropy of wavelet components and artificial neural networks*, 2013 9th IEEE International Symposium on Diagnostics for Electric Machines, Power Electronics and Drives (SDEMPED), 27-30 Aug. 2013, 2013; pp 538-543.
18. Smith, W.A.; Randall, R.B. Rolling element bearing diagnostics using the case western reserve university data: A benchmark study. *Mechanical Systems and Signal Processing* **2015**, *64-65*, 100-131.
19. Kuo, Y.-C.; Hsieh, C.-T.; Yau, H.-T.; Li, Y.-C. Research and development of a chaotic signal synchronization error dynamics-based ball bearing fault diagnostor. *Entropy* **2014**, *16*.
20. Jha, A.G.; Das, A.P.; Abhinav, K. In *Effects of electromagnetic interference on non-autonomous chaotic circuits*, 2009 4th International Conference on Computers and Devices for Communication (CODEC), 14-16 Dec. 2009, 2009; pp 1-4.
21. Case western reserve university bearing data center. Available online: . http://csegroups.case.edu/bearingdatacenter/pages/welcome-case-western-reserve-university-bearing-data-center-website (accessed on 13 05 2018),
22. Su, H.; Zhao, F. *Chaos detection method for power quality disturbance*. 2006; Vol. 1.
23. Wang, M.H. Application of extension theory to vibration fault diagnosis of generator sets. *IEE Proceedings - Generation, Transmission and Distribution* **2004**, *151*, 503-508.
24. Mang-Hui, W.; Chih-Yung, H. Application of extension theory to pd pattern recognition in high-voltage current transformers. *IEEE Transactions on Power Delivery* **2005**, *20*, 1939-1946.
25. Mang-Hui, W. Extension neural network-type 2 and its applications. *IEEE Transactions on Neural Networks* **2005**, *16*, 1352-1361.